

DOI: 10.1002/cssc.201300774

# Catalytic Transfer Hydrogenation/Hydrogenolysis for Reductive Upgrading of Furfural and 5-(Hydroxymethyl)furfural

David Scholz, Christof Aellig, and Ivo Hermans\*<sup>[a]</sup>

The sequential transfer hydrogenation/hydrogenolysis of furfural and 5-hydroxymethylfurfural to 2-methylfuran and 2,5-dimethylfuran was studied over in situ reduced, Fe<sub>2</sub>O<sub>3</sub>-supported Cu, Ni, and Pd catalysts, with 2-propanol as hydrogen donor. The remarkable activity of Pd/Fe<sub>2</sub>O<sub>3</sub> in both transfer hydrogenation/hydrogenolysis is attributed to a strong metal-support

interaction. Selectivity towards hydrogenation, hydrogenolysis, decarbonylation, and ring-hydrogenation products is shown to strongly depend on the Pd loading. A significant enhancement in yield to 62%, of 2-methylfuran and 2-methyltetrahydrofuran was observed under continuous flow conditions.

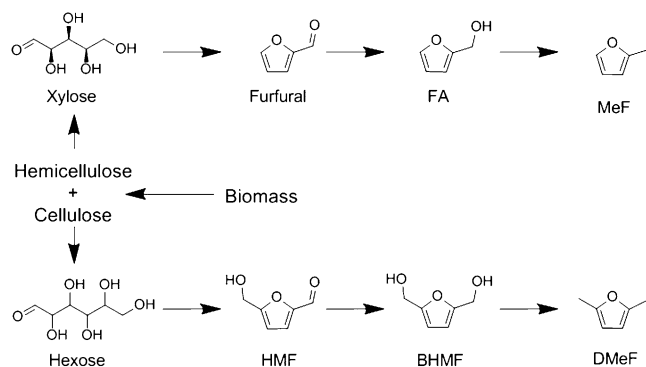
## Introduction

The reductive upgrading of biomass-derived platform molecules has recently gained increased attention as a strategy for the sustainable production of feedstocks for the chemical industry.<sup>[1]</sup> In particular, the selective hydro-deoxygenation of furanic aldehydes (Scheme 1) such as furfural and 5-(hydroxymethyl)furfural (HMF) to 2-methylfuran (MeF) and 2,5-dimethylfuran (DMeF) exhibits great potential for production of liquid fuel-substitutes from renewable substrates. Both furfural and HMF may be obtained from the acid-catalyzed dehydration of hemicellulose and cellulose-derived carbohydrates.<sup>[2]</sup> MeF and

DMeF offer beneficial physical and chemical properties for application as biofuels; an approximately 40% greater energy density (31.2 MJ kg<sup>-1</sup>, 35 MJ kg<sup>-1</sup>) than ethanol, high research octane numbers (RON = 131, RON = 119), and little-to-no solubility in water (7.0 g L<sup>-1</sup>, 2.3 g L<sup>-1</sup>).<sup>[3]</sup>

In the presence of hydrogen, the hydrodeoxygenation of furfural and HMF to the corresponding methylfurans may be accomplished over various supported noble metal and bimetallic catalysts.<sup>[4,5]</sup> The hydrodeoxygenation occurs via the intermediate alcohol species, furfuryl alcohol (FA) and 2,5-bis(hydroxymethyl)furan (BHMF) that are formed through hydrogenation and, subsequently, undergo hydrogenolysis. Common hydrogenation/hydrogenolysis catalysts include (Pd,<sup>[6]</sup> Pt,<sup>[4e]</sup> Ru, Rh),<sup>[4c]</sup> Cu,<sup>[5a-b]</sup> and (Ni, Fe).<sup>[5d]</sup> Cu-based catalysts have proven to exhibit exceptional activity in the cleavage of C–O bonds. Yields in DMeF of 61% and 79% were reported by Dumesic et al.,<sup>[4a]</sup> employing copper supported on chromite (CuCrO<sub>4</sub>) and carbon-supported bimetallic copper–ruthenium (CuRu/C) catalysts. More recently, the activity of bimetallic Ni–Fe catalysts in the C–O cleavage of furfural was demonstrated, achieving 39% yield in MeF.<sup>[5d]</sup> Furthermore, Pd has been shown to be active in the hydrogenation/hydrogenolysis of aromatic carbonyls and alcohols.

Despite the technical viability of reductive upgrading strategies for biomass utilization, the employment of molecular hydrogen presents a number of challenges for process economics and sustainability. On this basis, reductive upgrading employing alternative hydrogen donors such as formic acid and alcohols has recently gained increased attention. The catalytic transfer hydrogenation/hydrogenolysis of benzyl-alcohols with formic acid can be catalyzed by Pd catalysts.<sup>[7]</sup> Thananathana-chon et al. reported on the highly efficient production of DMeF from HMF, obtaining 95% yield when employing formic acid, H<sub>2</sub>SO<sub>4</sub>, and Pd/C in THF.<sup>[8]</sup> Despite the obvious advantages in storage, handling, and transport as compared to hydrogen, the corrosiveness of formic acid poses significant challenges to



**Scheme 1.** Schematic of the reductive upgrading pathway for biomass derived xyloses and hexoses. FA: furfuryl alcohol, MeF: 2-methylfuran, HMF: 5-(hydroxymethyl)furfural, BHMF: 2,5-bis(hydroxymethyl)furan, DMeF: 2,5-dimethylfuran.

[a] D. Scholz, C. Aellig, Prof. Dr. I. Hermans  
Institute for Chemical and Bioengineering  
ETH Zürich  
Wolfgang-Pauli-Strasse 10, 8093 Zürich (Switzerland)  
Fax: (+41) 44-633-42-58  
E-mail: hermans@chem.ethz.ch

Supporting Information for this article is available on the WWW under <http://dx.doi.org/10.1002/cssc.201300774>.

material and catalysts durability. Utilization of alcohols as hydrogen donors in catalytic transfer hydrogenation/hydrogenolysis reactions has been investigated under application of different catalysts and substrates. DMeF was produced with yields of up to 80% by employing Ru/C and 2-propanol as donor.<sup>[9]</sup> However, because of the deactivation of the Ru/C catalysts, further studies are currently being performed to investigate the nature of the deactivation phenomena. Armstrong et al. demonstrated the activity of Raney-nickel and cobalt in the catalytic transfer hydrogenolysis of aromatic alcohols.<sup>[10]</sup> Additionally, much effort has been devoted to improving the understanding and performance of catalysts in the hydrogenolysis of glycerol. Güemez et al. applied Ni-Cu/Al<sub>2</sub>O<sub>3</sub> catalysts in the hydrogenolysis of glycerol to 1,2-propanediol using 2-propanol or methanol as hydrogen donor.<sup>[11]</sup> More recently, Pietropaolo et al. obtained 94% yield in 1,2-propanediol when applying unreduced Pd/Fe<sub>2</sub>O<sub>3</sub> to a solution of glycerol in 2-propanol.<sup>[12]</sup>

Herein, we report on the catalytic transfer hydrogenation/hydrogenolysis of furfural and HMF, applying Ni-, Cu-, and Pd-supported catalysts, under batch as well as continuous flow reactions conditions.

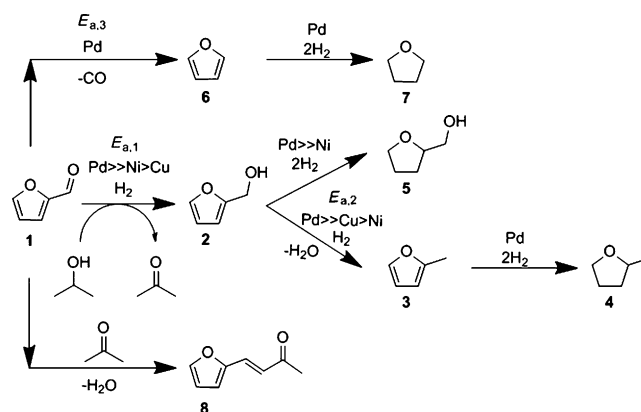
## Results and Discussion

### Transfer hydrogenation/hydrogenolysis of furfural

Initial experiments focused on the activity of Ni-, Cu-, and Pd-supported catalysts in the catalytic transfer hydrogenation/hydrogenolysis of furfural (1). For this purpose, 10 wt% Cu/Fe<sub>2</sub>O<sub>3</sub>, 10 wt% Ni/Fe<sub>2</sub>O<sub>3</sub>, and 10 wt% Pd/Fe<sub>2</sub>O<sub>3</sub> catalysts were synthesized by co-precipitation (see Experimental Section). In a typical experiment, the autoclave was charged with furfural, an internal standard, 2-propanol, and the catalyst. The molar ratio of substrate to catalyst was 175:1. The weight of Cu, Ni, and Pd catalyst charged into the reactor was adjusted such that the number of moles of metal remained constant over the experiments. The primary product of the transfer hydrogenation was FA (2). The successive hydrogenolysis of the hydroxyl group yields 2-methylfuran (3). In parallel to hydrogenation, furfural may undergo decarbonylation to furan (6). With increasing conversion (and hence, increasing concentration of acetone) the aldol-condensation product of furfural and acetone, 4-(furan-2-yl)but-3-en-2-one (8) is detected. Furthermore, we detected traces of furan-ring hydrogenation products, 2-methyl-tetrahydrofuran (THMeF, 4), (tetrahydrofuran-2-yl)methanol (THFA, 5), and tetrahydrofuran (THF, 7).

To verify that 2-propanol served as hydrogen donor in the catalytic transfer hydrogenation/hydrogenolysis to furfural, the acetone concentration was monitored (see the Supporting Information, Figure S2). In the initial phase of the reaction, in which FA was the main product, we found that approximately 1 equivalent of acetone was formed per equivalent of FA.

The main product over Cu and Ni was FA. Cu and Ni exhibited limited activity in the further hydrogenolysis to MeF. Products of the ring hydrogenation and decarbonylation reaction were not detected (Table 1). Scheme 2 shows the reaction pathways catalyzed by Cu, Ni, and Pd. The differences in the



**Scheme 2.** Reaction pathway for the catalytic transfer hydrogenation/hydrogenolysis of furfural employing Ni/Fe<sub>2</sub>O<sub>3</sub>, Cu/Fe<sub>2</sub>O<sub>3</sub>, and Pd/Fe<sub>2</sub>O<sub>3</sub>. Reactivity order of metals is based on the obtained yields of the respective product under the chosen reaction conditions.

**Table 1.** Catalytic transfer hydrogenation/hydrogenolysis of furfural over different metal catalysts.<sup>[a]</sup>

Catalyst	Conversion [%]		Yield [%]		
	1	2	3	6	4, 5, 7
Cu/Fe <sub>2</sub> O <sub>3</sub>	37	28	0	0	0
Ni/Fe <sub>2</sub> O <sub>3</sub>	46	33	0	0	0
Pd/Fe <sub>2</sub> O <sub>3</sub>	68	41	4	7	< 1

[a] Reaction conditions: furfural (0.40 M) in 2-propanol (40 mL), with 10 wt% Cu, Ni, or Pd/Fe<sub>2</sub>O<sub>3</sub> under N<sub>2</sub> atmosphere and 180 °C. Conversion and yield values were ascertained at the end of the reaction after 7.5 h.

reactivity behavior of Cu, Ni, and Pd catalysts in transfer hydrogenation/hydrogenolysis, decarbonylation, and ring-hydrogenation reactions are a result of preferential stabilization of the intermediate species by the different metal atoms. Previous studies have demonstrated that the hydrogenation of furfural over Cu catalysts occurs through coordination of the carbonyl group, in a η<sup>1</sup>(O)-aldehyde configuration.<sup>[5b,13]</sup> This rationalizes the observation that the main product over Cu/Fe<sub>2</sub>O<sub>3</sub> was FA, which was obtained with 75% selectivity. Ring-hydrogenated products (4, 5, 7) were not formed. Despite previous reports on the H<sub>2</sub>-mediated hydrogenation of furfural over Ni-catalysts, yielding primarily decarbonylation, ring-opening, and ring-hydrogenation products,<sup>[5a]</sup> we obtained FA as the primary product with 73% selectivity.

In contrast to Cu and Ni, Pd displayed activity in the hydrogenation of the furan-ring producing (4, 5, 7). Furan derivatives may coordinate through the π-system of the ring, allowing the formation of ring-hydrogenated products.<sup>[5a,14]</sup> In contrast, hydrogenation of the oxo functionalities occurs via formation of η<sup>2</sup>(C,O)-aldehydes, in which both the C and O atom are coordinated to Pd atoms. The η<sup>2</sup>-aldehyde may transform into a more stable surface acyl-species, which is known to be an intermediate in the decarbonylation, yielding furan.<sup>[5a]</sup> FA, MeF, and furan were formed with 61%, 7%, and 11% selectivity. The selectivity towards the ring hydrogenation products (4, 5,

7) was below 1%. The yield of the aldol condensation product (8) was below 1% for all tested catalysts.

Further on, the different activities of Cu, Ni, and Pd catalysts in the hydrogenation/hydrogenolysis reaction will be directly defined by the degree of reduction accomplished under reaction conditions. Temperature-programmed reduction profiles from the literature suggest that complete reduction of metallic species may only be accomplished for Pd.

The H<sub>2</sub>-temperature-programmed reduction (TPR) profile of Cu/Fe<sub>2</sub>O<sub>3</sub> and Ni/Fe<sub>2</sub>O<sub>3</sub> both exhibit two maxima, at 171 and 210 °C, and 277 and 318 °C, respectively. In contrast, Pd/Fe<sub>2</sub>O<sub>3</sub> exhibits a single reduction maximum at 113 °C (Figure S17). It is, therefore, believed that Pd(II) is almost completely reduced to Pd<sup>0</sup> under reaction conditions. On the other hand, only a fraction of the Cu and the Ni species will be reduced under the chosen reaction conditions. However, we emphasize that the H<sub>2</sub>-TPR measurements show that the consumption of H<sub>2</sub> begins at a temperature of 100 °C for Cu/Fe<sub>2</sub>O<sub>3</sub> and Ni/Fe<sub>2</sub>O<sub>3</sub>. This observation can likely be ascribed to the reduction of the metal species, which are highly dispersed and/or subject to strong interactions with the support. Furthermore, reduction maxima for Cu/Fe<sub>2</sub>O<sub>3</sub> and Ni/Fe<sub>2</sub>O<sub>3</sub> are shifted to lower temperatures as compared to Cu/SiO<sub>2</sub> (335 and 246 °C<sup>[5b]</sup>) and Ni/SiO<sub>2</sub> (354 °C<sup>[15]</sup>).

The occurrence of an induction period, as can be seen in Figures 1, 2, and 3, can likely be ascribed to the in situ formation of metallic species. X-ray photoelectron spectroscopy

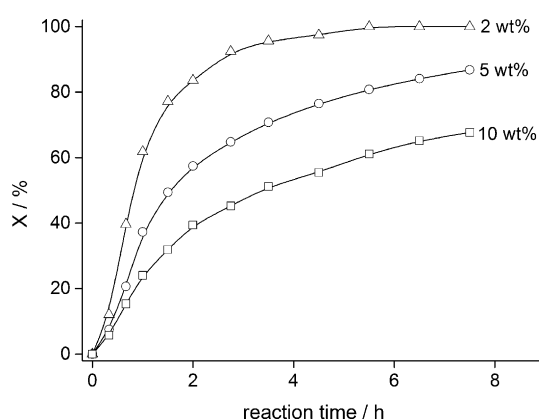


**Figure 1.** Conversion of furfural over different Pd loadings on Fe<sub>2</sub>O<sub>3</sub>. Reaction conditions: furfural (0.40 M) in 2-propanol (40 mL) with Pd/Fe<sub>2</sub>O<sub>3</sub> (10 wt%, 100 mg), Pd/Fe<sub>2</sub>O<sub>3</sub> (5 wt%, 200 mg) and Pd/Fe<sub>2</sub>O<sub>3</sub> (2 wt%, 500 mg) under N<sub>2</sub> atmosphere and 180 °C.

(XPS) measurements of the fresh and used Pd catalyst clearly confirm the in situ reduction of the Pd species (Figures S15 and 16). The Pd 3d<sub>5/2</sub> binding energy of the fresh sample is 337.4 eV, whereas a shift towards lower binding energies is observed for the used catalyst (335.1–335.5 eV), indicating a reduction of Pd(II) to Pd<sup>0</sup>. The binding energy of the Fe 2p<sub>3/2</sub> (710.6 eV) and Fe 2p<sub>1/2</sub> (724 eV) transition are consistent with published values for the hematite structure of the support.<sup>[16]</sup> A minor decrease in the binding energies of the Fe 2p<sub>3/2</sub> and Fe 2p<sub>1/2</sub> transition was observed for the used Pd catalyst.

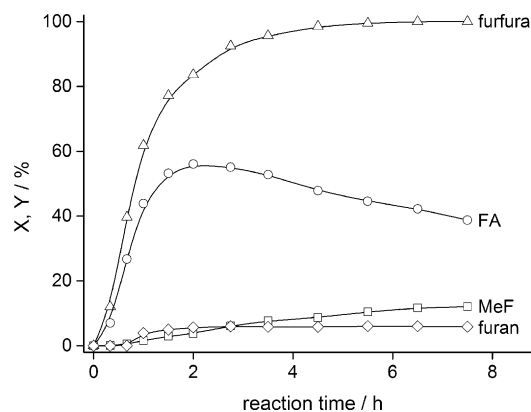


**Figure 2.** Conversion and yields in the catalytic transfer hydrogenation of 2-propanol to furfural over 2 wt% Pd/Fe<sub>2</sub>O<sub>3</sub>. Reaction conditions: furfural (0.40 M) in 2-propanol (40 mL) with Pd/Fe<sub>2</sub>O<sub>3</sub> (500 mg, 2 wt%) under N<sub>2</sub> atmosphere and 180 °C. Conversion: furfural; yields: FA, furan, MeF.

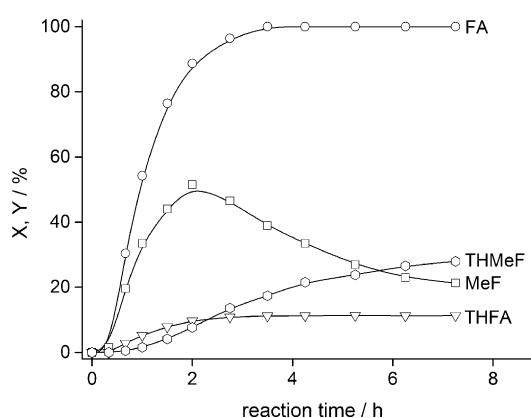


**Figure 3.** Conversion of FA over 10 wt% Pd/Fe<sub>2</sub>O<sub>3</sub>. Reaction conditions: FA (0.40 M) in 2-propanol (40 mL) with Pd/Fe<sub>2</sub>O<sub>3</sub> (100 mg, 10 wt%) under N<sub>2</sub> atmosphere and at 180 °C. Conversion: FA; yields: MeF, THMeF, THFA.

The active surface area of the 2 wt% Pd/Fe<sub>2</sub>O<sub>3</sub> catalyst was calculated from the amount of CO desorbed after saturation adsorption to be  $S_{act} = 3.9 \text{ m}^2 \text{ g}^{-1}$ .

To optimize the activity, as well as selectivity, in the formation of MeF, we investigated the reactivity of Pd/Fe<sub>2</sub>O<sub>3</sub> catalysts with loadings of 2, 5, and 10 wt% (Table 2). For comparative purposes, the catalyst amount was altered over the experiments so that the number of moles of Pd remained constant.

**Table 2.** Catalytic transfer hydrogenation/hydrogenolysis of furfural over Pd catalysts.

Catalyst	Conversion [%]		Yield [%]	
	1	2	3	6
10 wt% Pd/Fe <sub>2</sub> O <sub>3</sub> <sup>[a]</sup>	68	41	4	7
5 wt% Pd/Fe <sub>2</sub> O <sub>3</sub> <sup>[a]</sup>	87	57	10	8
2 wt% Pd/Fe <sub>2</sub> O <sub>3</sub> <sup>[a]</sup>	100	34	13	5
2 wt% Pd/Fe <sub>2</sub> O <sub>3</sub> <sup>[b]</sup>	71	32	1	6
2 wt% Pd/Fe <sub>2</sub> O <sub>3</sub> <sup>[c]</sup>	66	37	1	5
10 wt% Pd/C <sup>[a]</sup>	22	5	0	6

[a] Reaction conditions: furfural (0.40 M) in 2-propanol (40 mL) under N<sub>2</sub> atmosphere and 180 °C. Conversion and yield values were ascertained at the end of the reaction after 7.5 h. [b] 165 °C. [c] 150 °C.

As can be seen in Figure 1, 2 wt% Pd/Fe<sub>2</sub>O<sub>3</sub> demonstrated the highest activity in the catalytic transfer hydrogenation. We attribute the trend in catalytic activity to the morphology adopted by Pd particles and their interaction with the hematite (Fe<sub>2</sub>O<sub>3</sub>) support. The activation of O–H in H-donors is likely to require intimate contact between Pd and Fe species. The oxophilic nature of Fe<sup>[5d]</sup> promotes coordination of the oxofunctionality, promoting activation of the O–H bond. STEM measurements confirmed that Pd forms nano-crystalline structures with a particle size of 1–6 nm (Figures S9–12). Likewise, the support formed crystallites on a nanoscopic scale. With increasing loading and a general tendency towards formation of larger Pd agglomerates, the proportion of Pd atoms in direct proximity to the support is reduced. Furthermore, the selectivity towards MeF decreased while the furan selectivity increased with increasing Pd loading. The activity of Pd in the cleavage of C–C bonds (decarbonylation) is well described in literature.<sup>[5a–c]</sup> We thus expected a higher selectivity towards furan with increasing Pd loading, that is, Pd particle size. The premise of decarbonylation occurring primarily on Pd sites is confirmed by the determined activation barrier. The measured activation barrier of  $E_{a,3} = 16.8 \pm 1 \text{ kcal mol}^{-1}$  (Figure S7) is in good agreement with that reported,  $17 \text{ kcal mol}^{-1}$  over Pd.<sup>[17]</sup> Additionally, an experiment utilizing commercial 10 wt% Pd/C delivered furan and FA with 30% and 24% selectivity, respectively. No products of the hydrogenolysis reaction could be detected. It was recently suggested that Pd exhibits no stand-alone activity in the hydrogenolysis of FA.<sup>[17]</sup> However DFT calculations indicate that the C–O cleavage of FA over Pd–Fe sites may occur with an activation barrier of  $23 \text{ kcal mol}^{-1}$ .<sup>[17]</sup> The reported activation energy is in good agreement with that determined,  $E_{a,2} = 22.6 \pm 1 \text{ kcal mol}^{-1}$  (Figure S5).<sup>[17]</sup> It is, therefore, believed that the reactivity behavior of Pd/Fe<sub>2</sub>O<sub>3</sub> in the hydrogenolysis of FA is based on strong interactions between Pd and the support. The determined activation energy for the transfer hydrogenation yielding FA was  $E_{a,1} = 11.2 \pm 1 \text{ kcal mol}^{-1}$ .

### Transfer hydrogenolysis of FA

To gain a better understanding of the reaction dynamics occurring in the hydrogenation of furfural and subsequent hydrogenolysis to MeF, we focused our attention on investigating the C–O cleavage over different metal catalysts, loadings, and supports. The transfer hydrogenolysis of FA over Pd/Fe<sub>2</sub>O<sub>3</sub> occurs at temperatures as low as 150 °C. Initial experiments were, as before, conducted in an autoclave which was charged with FA, an internal standard, 2-propanol, and the catalyst. Both 10 wt% Cu/Fe<sub>2</sub>O<sub>3</sub> and 10 wt% Ni/Fe<sub>2</sub>O<sub>3</sub> showed limited-to-no activity in the hydrogenolysis of FA. In comparison with previous experiments, the catalytic transfer hydrogenolysis of FA over Pd/Fe<sub>2</sub>O<sub>3</sub> yielded notable amounts of ring-hydrogenated products (Table 3).

The catalytic transfer hydrogenation/hydrogenolysis utilizing 10 wt% Pd/Fe<sub>2</sub>O<sub>3</sub> formed THFA, MeF, and THMeF with 11%, 21%, and 28% selectivity, respectively. Figure 3 demonstrates the sequential transformation of FA to MeF, which is further hydrogenated to yield THMeF. As confirmed in a separate ex-

**Table 3.** Catalytic transfer hydrogenolysis of FA over different catalysts.

Catalyst	Conversion [%]		Yield [%]	
	1	4	5	7
10 wt% Cu/Fe <sub>2</sub> O <sub>3</sub> <sup>[a]</sup>	7	1	0	0
10 wt% Ni/Fe <sub>2</sub> O <sub>3</sub> <sup>[a]</sup>	9	0	<1	<1
10 wt% Pd/Fe <sub>2</sub> O <sub>3</sub> <sup>[a]</sup>	100	21	28	11
2 wt% Pd/Fe <sub>2</sub> O <sub>3</sub> <sup>[a]</sup>	99	31	9	17
2 wt% Pd/Fe <sub>2</sub> O <sub>3</sub> <sup>[b]</sup>	95	42	5	24
2 wt% Pd/Fe <sub>2</sub> O <sub>3</sub> <sup>[c]</sup>	69	39	2	33
1 wt% Pd/Fe <sub>2</sub> O <sub>3</sub> <sup>[a]</sup>	99	35	9	25
10 wt% Pd/C <sup>[a]</sup>	7	5	0	0
10 wt% Pd/Al <sub>2</sub> O <sub>3</sub>	10	8	0	0
10 wt% Pd/MgO	13	2	0	0

[a] Reaction conditions: FA (0.40 M) in 2-propanol (40 mL) under N<sub>2</sub> atmosphere and 180 °C. Conversion and selectivity values were ascertained at the end of the reaction after 7.5 h. [b] 165 °C. [c] 150 °C.

periment, the THFA formed in parallel shows no further reactivity in the hydrogenolysis to THMeF.

As mentioned previously, the occurrence of ring hydrogenation products may be explained by the tendency of furfural derivatives to coordinate to Pd through the  $\pi$ -system of the furan ring. The fact that THFA does not undergo hydrogenolysis suggests that the presence of the  $\pi$ -system is essential for the formation of the transition state yielding MeF. To reduce the formation of ring-hydrogenated products that promote excessive hydrogen consumption, we investigated the reactivity behavior of different Pd loadings. At lower Pd loadings, we observed a reduced tendency of MeF to undergo ring hydrogenation (Figure S3). Various studies have indicated that the hydrogenation of unsaturated hydrocarbons over Pd exhibits a decrease in specific activity with increasing metal dispersion, especially over small particle sizes.<sup>[20]</sup> It is, therefore, possible that the increased formation of ring-hydrogenated products over higher Pd loadings may be a direct consequence of the presence of larger particle sizes (Figures S9–12). Table 3 provides a summary of the results obtained for the hydrogenolysis of FA over various metal catalysts. The low activity of Pd/C, Pd/MgO, and Pd/Al<sub>2</sub>O<sub>3</sub> in the catalytic transfer hydrogenolysis further supports the hypothesis that the reactivity of Pd/Fe<sub>2</sub>O<sub>3</sub> arises from a strong metal–support interaction. Similar conclusions have been established by Huber et al. who attributed the extraordinary activity of Pd/Fe<sub>3</sub>O<sub>4</sub> in aqueous phase reforming of ethylene glycol to the synergistic effect of Pd nanoparticles and magnetite (Fe<sub>3</sub>O<sub>4</sub>).<sup>[18]</sup> We emphasize that a blank experiment employing only the Fe<sub>2</sub>O<sub>3</sub> support showed no activity towards formation of MeF.

### Donor capability of different alcohols

The coupling of the transfer hydrogenation/hydrogenolysis reaction with a specific donor allows for efficient production of the carbonyl form of the alcohol as a side product of the process. To examine the donor capabilities of alcohols, primary and secondary alcohols with different carbon chain lengths were tested. It was found that donor capability decreases with carbon-chain length of the alcoholic species, and, in particular,

Donor	Product	Conversion [%] (2)	Yield [%] (3+4)
		99	37
		52	45
		97	49
		27	48

[a] Reaction conditions: FA (0.40 M) in alcohol (40 mL) under N<sub>2</sub> atmosphere and 180 °C. Conversion and selectivity values were ascertained at the end of the reaction after 7.5 h.

with degree of substitution of the alcohol. Of the tested alcohols, 2-propanol demonstrated the highest activity (Table 4). These findings are in agreement with the literature, which generally reports that secondary alcohols have a higher tendency to release hydrogen than primary alcohols.<sup>[19]</sup>

#### Transfer hydrogenation/hydrogenolysis of furfural under continuous flow conditions

For further optimization/intensification of the obtained yields in MeF, as well as testing of the catalysts stability, we progressed to studying the transfer hydrogenation/hydrogenolysis of both furfural and FA in a continuous-flow reactor. In comparison with conventional batch reactors, continuous-flow reactors provide a number of advantages including improved productivity, enhanced heat and mass transfer, and smaller reactor volumes.<sup>[2c]</sup> The reactor system consisted of a HPLC pump that introduced the liquid feed (0.40 M furfural or FA, 2-propanol, and an internal standard), into a stainless steel tubular reactor (46 mm internal diameter). The pressure over the system was controlled through a back-pressure regulator installed at the outlet of the reactor.

The reactor was densely packed with the 2 wt% Pd/Fe<sub>2</sub>O<sub>3</sub> catalyst diluted with quartz (ratio of 25:75 by weight). Figure 4 shows the concentration profiles in the transfer hydrogenation/hydrogenolysis of furfural under these continuous flow conditions.

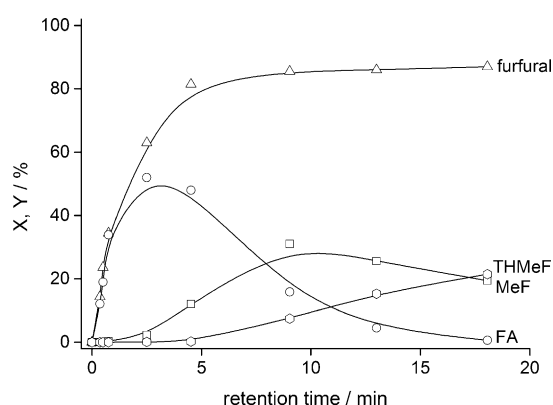


**Figure 4.** Continuous transfer hydrogenation/hydrogenolysis of furfural. Reaction conditions: furfural (0.40 M) in 2-propanol with Pd/Fe<sub>2</sub>O<sub>3</sub> (2.5 g, 2 wt%) at 25 bar pressure and 180 °C. Conversion: furfural; yields: FA, MeF, THMeF.

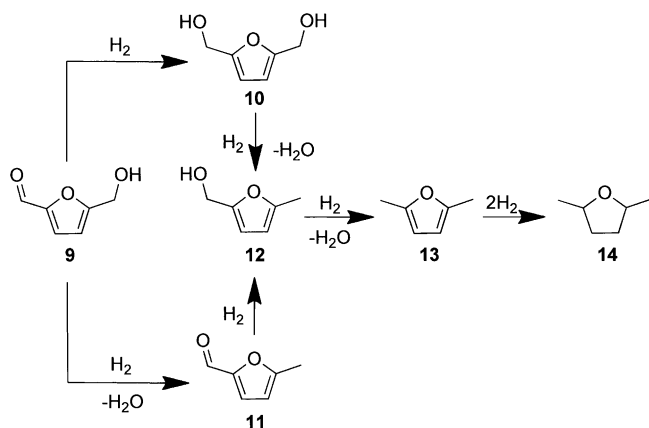
tion/hydrogenolysis of furfural under these continuous flow conditions. Unlike in previous batch experiments, we obtained notable amounts of ring-hydrogenated products of MeF and FA. In previous batch experiments, these had only been detected in trace amounts when employing furfural as substrate. At the longest residence time, MeF, THMeF, THFA, and furan were formed with 19%, 21%, 29%, and 2% yield, respectively. At intermediary residence times, FA is obtained with 70% selectivity at 81% conversion. The accelerated formation of hydrogenolysis and ring-hydrogenated products indicates the presence of a competitive adsorption equilibrium between different species in the reaction system. In fact, Figure 4 indicates that the formation of MeF is inhibited as long as furfural is present in the system. DFT calculations suggested that the heat of adsorption of furfural on noble metals is significantly larger than that of FA and MeF.<sup>[5b,c,17]</sup> This suggests that the catalyst surface is effectively saturated with furfural until near completion of the transfer hydrogenation, at which point the adsorption and hydrogenolysis of FA is accelerated. Figure 4 shows that the formation rate of MeF is drastically accelerated as furfural conversion approaches 100%. The same observation applies to the formation rate of THFA. Conducting the transfer hydrogenation/hydrogenolysis at lower substrate concentrations (0.12 M furfural), promotes a significant enhancement in yield of MeF and THMeF to 62%. MeF, THMeF, THFA, and furan were formed with 26%, 36%, 24%, and <1% selectivity. During operation of the system at near-full conversion, the evolution of notable gas amounts is observed. We attribute the gas evolution to the continued dehydrogenation of 2-propanol.

The continuous-flow transfer hydrogenolysis of FA exhibited a significant enhancement in the yield: 76% of MeF as compared with 31% under batch conditions. Furthermore, the formation of ring-hydrogenation products was reduced to 4% yield in THFA and 2% THMeF. The lower yield in ring-hydrogenation products of MeF, as compared with batch experiments, is explained by the reduced contact time with the catalyst.

To determine the presence of competitive adsorption equilibrium between furfural and FA, and its effect on the formation of MeF and THFA, we conducted a continuous-flow experiment in which the feed was enriched incrementally with furfural. To the initial feed of 0.40 M FA in 2-propanol, was added 1 mol% furfural and, subsequently, 5 mol% (total) furfural (based on moles of FA). Upon addition of 1 mol% furfural, the yield in MeF decreased from 60% to 57%. Further addition of furfural up to a total of 5 mol% promoted a further reduction in the yield to 49%. After switching the feed again to pure FA, the system exhibited a lag time of 40 min until the yield in MeF again approached its starting value. The reversibility of the process is a further indication of the presence of adsorption equilibrium. With the use of the continuous-flow reactor setup we also conducted a stability test of the catalyst under reaction conditions over 47 h (Figure S8). Under reaction conditions, the catalyst exhibited an initial activity achieving 50% conversion in furfural. After 20 h, furfural conversion had decreased to 40%, at which it stabilized for the remainder of the measurement interval.

## Transfer hydrogenation/hydrogenolysis of HMF under continuous flow conditions

The transfer hydrogenation/hydrogenolysis of HMF (**9**, Scheme 3) was conducted in a continuous-flow reactor setup. The deoxygenation reaction of HMF proceeds via the inter-



**Scheme 3.** Reaction pathway for the catalytic transfer deoxygenation of HMF.

mediate BHMf (**10**), which undergoes hydrogenolysis to DMef (**13**). DMef may undergo ring hydrogenation, forming 2,5-dimethyltetrahydrofuran (THDMef, **14**). At low residence times and temperatures, we detected 5-methylfuran-2-carbaldehyde (**11**) as well as (5-methylfuran-2-yl)methanol (**12**), which originate from the transfer hydrogenation and transfer hydrogenolysis of HMF.

The deoxygenation of HMF yielded 72% DMef. Under the chosen reaction conditions (catalyst loading, residence times), the yield in THMeF was below 1%. However, at significantly longer residence times, DMef readily undergoes ring hydrogenation to form a mixture of (2*S*,5*S*)- and (2*R*,5*S*)-2,5-dimethyltetrahydrofuran. At short residence times and lower temperatures (150 °C), the intermediate BHMf is obtained with 70% selectivity at 50% conversion (Figure 5).

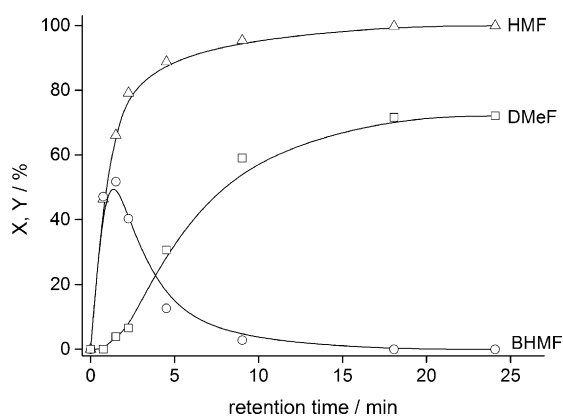


**Figure 5.** Continuous flow transfer hydrogenolysis of HMF. Reaction conditions: HMF (0.12 M) in 2-propanol with Pd/Fe<sub>2</sub>O<sub>3</sub> (1.6 g, 2 wt%) at 25 bar pressure and 180 °C. Conversion: HMF; yields: DMef, BHMf.

## Conclusions

The high proportion of oxy functionalities in biomass-derived platform molecules requires efficient methods for selective deoxygenation. In situ reduced Pd catalysts supported on Fe<sub>2</sub>O<sub>3</sub> allow for the transfer hydrogenation/hydrogenolysis of furanic aldehydes, utilizing alcohols as hydrogen donors. The formation of hydrogenation, hydrogenolysis, decarbonylation, and ring-hydrogenation products from furfural was demonstrated to exhibit a strong dependence on the employed metal. Unlike in the case of Pd, complete reduction of Cu and Ni species is not accomplished under the chosen reaction conditions. Nonetheless transfer hydrogenation/hydrogenolysis of furfural over Cu and Ni catalysts yielded FA with high selectivity (75% and 73%) at low conversion. Pd/Fe<sub>2</sub>O<sub>3</sub> exhibited extraordinary activity in the further hydrogenolysis to MeF, but also in the formation of ring-hydrogenation and decarbonylation products. The reactivity of Pd/Fe<sub>2</sub>O<sub>3</sub> in C–O cleavage reactions was attributed to a strong metal–support interaction. The activity and selectivity in the formation of FA, MeF, and furan showed a strong dependence on the Pd loading. 2 wt% Pd/Fe<sub>2</sub>O<sub>3</sub> demonstrated the highest activity in transfer hydrogenation to furfural and selectivity towards formation of MeF. Under continuous flow conditions, an improved combined yield of MeF and THMeF of 40% was obtained. The yield was further increased to 62% when employing lower substrate concentrations. The continuous hydrogenation/hydrogenolysis of HMF showed a high selectivity towards either BHMf or DMef depending on the residence time and the temperature. Additionally, the activity Pd/Fe<sub>2</sub>O<sub>3</sub>, after a short decrease in conversion at the beginning, remained stable over 47 h.

## Experimental Section

Furfural (Acros Organics, 99%), FA (Aldrich, 98%), tetrahydrofurfuryl alcohol (Fluka, > 99%), furan (Aldrich, 98%), 5-(hydroxymethyl)furfural (Sigma, 99%), and 2,5-bis(hydroxyl-methyl)-furan were quantified against dodecane as internal standard by using GC (HP-FFAP column, FID). 2-methylfuran (TCI, > 98%), 2-methyltetrahydrofuran (Acros, 99%), tetrahydrofuran (Acros, 99%), 2,5-dimethylfuran (Sigma, 99%), and 2,5-dimethyltetrahydrofuran (Aldrich, cis-trans, 98%) were quantified by GC equipped with a HP-5 column and FID detector.

## Synthesis of BHMf

NaBH<sub>4</sub> (1.2 g, 32 mmol) was slowly added to 5-(hydroxymethyl)furfural (2.0 g, 16 mmol) dissolved in dry methanol (16 mL) at 0 °C. The reaction was stirred at room temperature for 15 min, after which the methanol was evaporated under vacuum. Distilled water (4 mL) and 2 M HCl (5 mL) was added to the residue, which was subsequently extracted with 7 × 10 mL ethyl acetate. The organic phase was dried over MgSO<sub>4</sub>. After removal of ethyl acetate under reduced pressure, 2,5-bis(hydroxymethyl)furan was obtained as a yellowish solid (0.65 g, 55%).

### Catalyst synthesis

Cu/Fe<sub>2</sub>O<sub>3</sub> and Ni/Fe<sub>2</sub>O<sub>3</sub> catalysts were prepared by co-precipitation in aqueous solutions of Cu(NO<sub>3</sub>)<sub>2</sub>·3H<sub>2</sub>O or Ni(NO<sub>3</sub>)<sub>2</sub>·6H<sub>2</sub>O, and Fe(NO<sub>3</sub>)<sub>3</sub>·9H<sub>2</sub>O. Na<sub>2</sub>CO<sub>3</sub> was gradually added to a metal precursor solution (0.10 M) containing Fe(NO<sub>3</sub>)<sub>3</sub>·9H<sub>2</sub>O, under vigorous stirring, until the pH of the solution reached 9. After precipitation, the suspension was maintained at room temperature for 1 h while stirring. The precipitate was washed with 6 × 1 L distilled water and dried under air flow. The catalyst was then stored for 12 h at 110 °C under air. Pd/Fe<sub>2</sub>O<sub>3</sub> catalyst with different loadings was synthesized by in situ generation of [PdCl<sub>4</sub>]<sup>2-</sup> and co-precipitation with Fe(NO<sub>3</sub>)<sub>3</sub>·9H<sub>2</sub>O. PdCl<sub>2</sub> was dissolved in HCl (37 wt%) to generate a 0.10 M solution. The solution was diluted with water (30 mL) and Fe(NO<sub>3</sub>)<sub>3</sub>·9H<sub>2</sub>O was added. Na<sub>2</sub>CO<sub>3</sub> was added until the solution reached a pH of 9, at which it was maintained for 1 h. The precipitate was washed with 6 × 1 L distilled water, dried under air flow, and stored at 110 °C for 12 h. For synthesis of catalysts with different loadings, the amount of PdCl<sub>2</sub> added to the solution was adjusted. Mg(NO<sub>3</sub>)<sub>2</sub>·6H<sub>2</sub>O and Al(NO<sub>3</sub>)<sub>3</sub>·9H<sub>2</sub>O were used as precursors for the synthesis of Pd/MgO and Pd/Al<sub>2</sub>O<sub>3</sub>.

For the synthesis of 2 wt% Pd/Fe<sub>2</sub>O<sub>3</sub>, PdCl<sub>2</sub> (0.18 g, 1 mmol) was dissolved in HCl (37 wt%, 9.3 mL) and diluted with H<sub>2</sub>O (30 mL). After complete dissolution, Fe(NO<sub>3</sub>)<sub>3</sub>·9H<sub>2</sub>O (25 g, 62 mmol) was added to the solution under vigorous stirring. Through gradual addition of solid Na<sub>2</sub>CO<sub>3</sub> (28 g, 265 mmol) precipitation was induced. Subsequently, the suspension was stirred at room temperature for 1 h, washed with 6 × 1 L distilled water, dried under air flow and stored at 110 °C for 12 h.

### Batch experiments

The transfer hydrogenation/hydrogenolysis reactions were performed in 100 mL Parr stainless steel autoclaves equipped with PEEK (polyetheretherketon) inserts. In a typical experiment, the reactor was charged with furfural (or FA) (1.50 g), dodecane (0.3 g), 2-propanol (40 mL), and Pd/Fe<sub>2</sub>O<sub>3</sub> (2 wt%, 500 mg). The reactor was purged thoroughly with N<sub>2</sub>, and finally pressurized to 15 bar. The reactor was brought to the desired temperature by means of a heating jacket.

### Continuous flow experiments

The tubular reactor (4.6 mm inner diameter) was densely packed with a 25 wt% mixture of 2 wt% Pd/Fe<sub>2</sub>O<sub>3</sub> catalyst diluted with quartz (0.1–0.2 mm diameter, void fraction 0.55). The inlet of the reactor was connected to an HPLC pump, and the outlet to a back-pressure regulator. Prior to immersing the reactor in a silicon oil bath, the liquid feed was pumped into the reactor at a rate of 0.40 mL min<sup>-1</sup> over 15 min. After pressurizing the reactor to 25 bar to prevent evaporation of the solvent, the reactor was heated to 180 °C. Before beginning sampling, the reactor was maintained at 180 °C while pumping feed at 0.40 mL min<sup>-1</sup> for 1 h to ensure activation of the catalyst.

### Catalyst Characterization

The chemical composition of Cu/Fe<sub>2</sub>O<sub>3</sub>, Ni/Fe<sub>2</sub>O<sub>3</sub>, and Pd/Fe<sub>2</sub>O<sub>3</sub> catalysts was characterized by inductively-coupled plasma optical emission spectroscopy (HORIBA Ultra 2). The solid samples were prepared by dissolution in 37 wt% HCl. The determined weight percents were as follows: 10 wt% Cu/Fe<sub>2</sub>O<sub>3</sub>: 8.62%; 10 wt% Ni/

Fe<sub>2</sub>O<sub>3</sub>: 7.36%; 2 wt% Pd/Fe<sub>2</sub>O<sub>3</sub>: 1.96%; 5 wt% Pd/Fe<sub>2</sub>O<sub>3</sub>: 4.97%; 10 wt% Pd/Fe<sub>2</sub>O<sub>3</sub>: 9.61%.

Results of CHN elemental analysis (LECO CHN-900) of the as-prepared catalysts were as follows: 10 wt% Cu/Fe<sub>2</sub>O<sub>3</sub> (C:0.07% H:0.15% N:0.06%), 10 wt% Ni/Fe<sub>2</sub>O<sub>3</sub> (C:0.03% H:0.09% N:0.07%), 10 wt% Pd/Fe<sub>2</sub>O<sub>3</sub> (C:0.05% H:0.12% N:0.06)

CO-adsorption and H<sub>2</sub>-TPR of catalysts was performed using a THERMO TPDRO 1100. The active surface area (S<sub>act</sub>) of 2 wt% Pd/Fe<sub>2</sub>O<sub>3</sub> was measured based on CO desorption assuming a CO/Pd stoichiometry of 1 and a surface area of 7.87 × 10<sup>-20</sup> m<sup>2</sup> per Pd atom.<sup>[21]</sup> H<sub>2</sub> adsorbed on the surface of the catalyst after reduction was removed through heating the sample under N<sub>2</sub> at 130 °C for 1 h. After cooling to 35 °C, CO pulses were injected until the peak areas of the consecutive CO pulses were constant.

XPS analysis was performed using a Phi5000 VersaProbe spectrometer (ULVAC-PHI, INC.) equipped with a 180° spherical capacitor energy analyzer. Spectra were acquired at a base pressure of 5 × 10<sup>-8</sup> Pa by using a focused scanning monochromatic AlK<sub>α</sub> (1486.6 eV) X-ray source.

The microstructure of the catalysts was observed by means of a Hitachi HD2700CS STEM (aberration-corrected dedicated STEM, cold field-emission source, 200 kV).

### Acknowledgements

Financial support from the ETH Zürich is gratefully acknowledged by the authors. The authors would like to thank Dr. Frank Krumeich for help with the electron microscopy pictures.

**Keywords:** biomass · dimethylfuran · furfural · heterogeneous catalysis · hydrogenolysis

- [1] L. Hu, G. Zhao, W. Hao, X. Tang, Y. Sun, L. Lin, S. Liu, *RSC Adv.* **2012**, *2*, 11184–11206.
- [2] a) R. Karinen, K. Vilonen, M. Niemelä, *ChemSusChem* **2011**, *4*, 1002–1016; b) J. B. Binder, J. J. Blank, A. V. Cefali, R. T. Raines, *ChemSusChem* **2010**, *3*, 1268–1272; c) C. Aellig, I. Hermans, *ChemSusChem* **2012**, *5*, 1737–1742.
- [3] C. Wang, H. Xu, R. Daniel, A. Ghafourian, J. M. Herreros, S. Shuai, X. Ma, *Fuel* **2013**, *103*, 200–211.
- [4] a) Y. Román-Leshkov, C. Barrett, Z. Y. Liu, J. Dumesic, *Nature* **2007**, *447*, 982–986; b) G. Luijkx, N. Huck, F. van Rantwijk, L. Maat, H. van Bekkum, *Heterocycles* **2009**, *77*, 1037–1044; c) M. Chidambaram, A. T. Bell, *Green Chem.* **2010**, *12*, 1253–1262; d) J. Gallo, D. Alonso, M. Mellmer, J. Dumesic, *Green Chem.* **2013**, *15*, 85–90; e) E. D'Hondt, S. Van de Vyver, B. F. Sels, P. A. Jacobs, *Chem. Commun.* **2008**, 6011–6012.
- [5] a) S. Sitthisa, D. Resasco, *Catal. Lett.* **2011**, *141*, 784–791; b) S. Sitthisa, T. Sooknoi, Y. Ma, P. Balbuena, D. Resasco, *J. Catal.* **2011**, *277*, 1–13; c) S. Sitthisa, T. Pham, T. Prasomsri, T. Sooknoi, R. Mallinson, D. Resasco, *J. Catal.* **2011**, *280*, 17–27; d) S. Sitthisa, W. An, D. Resasco, *J. Catal.* **2011**, *284*, 90–101; e) R. Rao, T. Baker, M. Vannice, *Catal. Lett.* **1999**, *60*, 51–57; f) H. Zheng, Y. Zhu, B. Teng, Z. Bai, C. Zhang, H. Xiang, Y. Li, *J. Mol. Catal. A* **2006**, *246*, 18–23; g) J. Lessard, J. Morin, J. Wehrung, D. Magnin, E. Chornet, *Top. Catal.* **2010**, *53*, 1231–1234; h) J. Lange, E. van der Heide, J. Buijtenen, R. Price, *ChemSusChem* **2012**, *5*, 150–166; i) D. Manly, A. Dunlop, *J. Org. Chem.* **1958**, *23*, 1093–1095; j) W. Burnett, I. Johns, R. Holdren, R. Hixon, *Ind. Eng. Chem.* **1948**, *40*, 502–505.
- [6] K. Hattori, H. Sajiki, K. Hirota, *Tetrahedron* **2001**, *57*, 4817–4824.
- [7] a) S. Sawadjoon, A. Lundstedt, J. Samec, *ACS Catal.* **2013**, *3*, 635–642; b) X. Liu, G. Lu, Y. Guo, Y. Wang, X. Wang, *J. Mol. Catal. A* **2006**, *252*, 176–180; c) J. Feng, C. Yang, D. Zhang, J. Wang, H. Fu, H. Chen, X. Li, *Appl. Catal. A* **2009**, *354*, 38–43; d) N. Thakar, N. Polder, K. Djanashvili, H. van Bekkum, F. Kapteijn, J. Moulijn, *J. Catal.* **2007**, *246*, 344–350.
- [8] T. Thananathanachon, T. Rauchfuss, *Angew. Chem.* **2010**, *122*, 6766–6768; *Angew. Chem. Int. Ed.* **2010**, *49*, 6616–6618.

- [9] J. Jae, W. Zheng, R. Lobo, D. Vlachos, *ChemSusChem* **2013**, *6*, 1158–1162.
- [10] B. Gross, R. Mebane, D. Armstrong, *Appl. Catal.* **2001**, *219*, 281–289.
- [11] a) I. Gandarias, P. Arias, S. Fernandez, J. Requies, M. El Doukkali, M. Güemez, *Catal. Today* **2012**, *195*, 22–31; b) I. Gandarias, P. Arias, J. Requies, M. El Doukkali, M. Güemez, *J. Catal.* **2011**, *282*, 237–247.
- [12] M. Musolino, L. Scarpino, F. Mauriello, R. Pietropaolo, *Green Chem.* **2009**, *11*, 1511–1513.
- [13] A. Chambers, S. Jackson, D. Stirling, G. Webb, *J. Catal.* **1997**, *168*, 301–314.
- [14] M. Bradley, J. Robinson, D. Woodruff, *Surf. Sci.* **2010**, *604*, 920–925.
- [15] M. Ermakova, D. Ermakova, *Catal. Today* **2002**, *77*, 225–235.
- [16] J. Moulder, W. Stickle, P. Sobol, K. Bomben, *Handbook of X-Ray Photoelectron Spectroscopy*, Perkin-Elmer Corp., Eden Prairie, **1992**.
- [17] D. Resasco in *ACS Spring Conference*, “Combined Kinetics and DFT analysis of the hydrogenolysis of furfural and HMF over PdFe Alloys”, San Diego **2012**.
- [18] G. Huber, J. Shabaker, S. Evans, J. Dumesic, *Appl. Catal.* **2006**, *62*, 226–235.
- [19] M. Giliński, U. Ulkowska, *Catal. Lett.* **2010**, *141*, 293–299.
- [20] S. Hub, L. Hilaire, R. Touroude, *Appl. Catal.* **1988**, *36*, 307–322.
- [21] H. Dropsch, M. Baerns, *Appl. Catal. A* **1997**, *158*, 163–183.

---

Received: July 30, 2013

Revised: September 24, 2013

Published online on November 13, 2013